University of California
Irvine

Graphene & Carbon Nanotube Biosensors for Scanning Microwave Imaging of Isolated Mitochondria

THESIS

submitted in partial satisfaction of the requirements
for the degree of

MASTER OF SCIENCE

In Biomedical Engineering

By

Zahra Nemati

Thesis Committee:
Professor Peter J. Burke, Chair
Professor Marc Madou, Ph.D.
Associate Professor James P. Brody, Ph.D.

Table of Contents

Acknowledgements

I would like to thank Professor Peter Burke for his continuous support and mentorship. I would also like to thank Dr. Weiwei Zhou for helping me through this degree and teaching me many valuable skills and lessons. I also like to acknowledge my wonderful lab mates Phi Pham and Jinfeng Li for their tips throughout my research. This work would not have been possible without them.

I'd like to thank the prestigious UC Irvine Biomedical Engineering Department for being resourceful and allowing me this opportunity. Lastly, I am grateful for my family for their unwavering love and support.

ABSTRACT OF THE THESIS

Graphene & Carbon Nanotube Biosensors for Scanning Microwave Imaging of Isolated Mitochondria

By

Zahra Nemati

Master of Science in Biomedical Engineering

University of California, Irvine, 2017

Professor Peter J. Burke, Chair

Mitochondrial bioenergetics and its relationship to apoptosis, otherwise known as programmed cell death, has been the focus of numerous studies in the past, including cancer biology, neurodegenerative disorders, etc. Historically, mitochondrial functions, dysfunctions and their properties have been studied using millions of cells, via a series of molecular assays, and with high variability and heterogeneity within the mitochondrial populations under study. The rationale behind the methods used and developed in this thesis is to study these intricate organelles on micro and nano-scales, and on a single isolated vital mitochondrion capacity. Given the currently available nano technologies, it is now possible to design, optimize and develop platforms that would allow for such nano scale explorations of sub-cellular dynamics. Furthermore, we have attempted to optimize the design and deposition process of more pristine nanotube based biosensors. This process involved the testing and characterization of various types of filter papers, substrates and functionalization schemes, which were studied and will be the topic of research in future investigations.

Chapter 1: Introduction

1.1 Introduction to Mitochondria

Mitochondria, also known as cellular powerhouse, are perhaps one of the most important cellular organelles. They are double membrane bound organelles that are found in all eukaryotic cells. Number of mitochondria per cell varies considerably, even within the same cell and tissue types. They are the main generators of cellular energy in the form of ATP (adenosine-5'-triphosphate), are involved in regulation of cellular metabolism, signaling as well as apoptosis, otherwise known as programmed cell death. Any disruption in mitochondrial function would invariably lead to a number of chronic diseases and disorders, including cancer, cardiac dysfunction, metabolic as well as a slew of neurodegenerative disorders. Mitochondria also contain their own genome, separate from the nuclear DNA. Unfortunately, however, given the complex nature of these organelles, the links between many diseases or disorders thought to associate with mitochondria are not well understood despite substantial studies in this field.

1.2 Structure of Mitochondria

Mitochondria are "oval shaped" and are typically anywhere between 0.75 to 3 μm in diameter and cannot be imaged via traditional imaging techniques, unless specifically tagged with fluorescent dyes. They move and can change their exact shape through fission and fusion, a more recently studied process. They are comprised of two membranes and while the outer one defines the external shape, the inner membrane has many folds, otherwise known as cristae. These folds create a very high surface area, which are extremely important in mitochondrial function. The area enclosed by the cristae is known as the matrix, which contains the mitochondrial genome, enzymes of the

TCA cycles and other structures such as ribosomes and granules. Similar to the cell's lipid bilayer, the mitochondrial outer membrane is composed of a number of phospholipids and proteins, that play a pivotal role in the mitochondrial morphology maintenance, metabolic exchange and cytosolic communication and signaling. For example, the mitochondrial membrane protein, translocase of the outer membrane (TOM) regulates the passage of the proteins encoded in the nucleus and shuttled to the mitochondrial matrix. The inner membrane is relatively impermeable and only small molecules can pass through the inner membrane via translocase of inner membrane (TIM) protein.

Below is a basic outline of the mitochondrial structure.

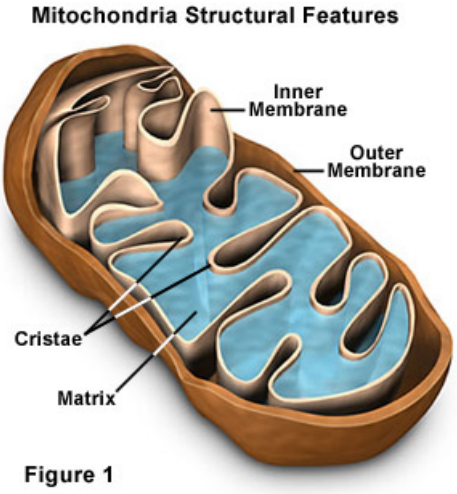

Figure 1

(1)

1.3 Membrane Potential of Mitochondria

The significance of the mitochondrial inner membrane lies in its ability to create an electrical potential by sequestering positive charges in the form of protons within the inner membrane space. This potential, better known physiologically as the proton-electromotive force, is essential for driving the ATP production of the electron transport chain, a series of protein complexes responsible for the bulk energy production within the cell. Since energy production is especially crucial for such cell types as the heart, brain and muscle cells, any decline in potential, or as a result, the energy production, can adversely impact the function of these systems. Hence, studying the changes and the influencers of the mitochondrial membrane potential ($\Delta\Psi_m$) is a critical step towards understanding the molecular mechanisms of many disorders.

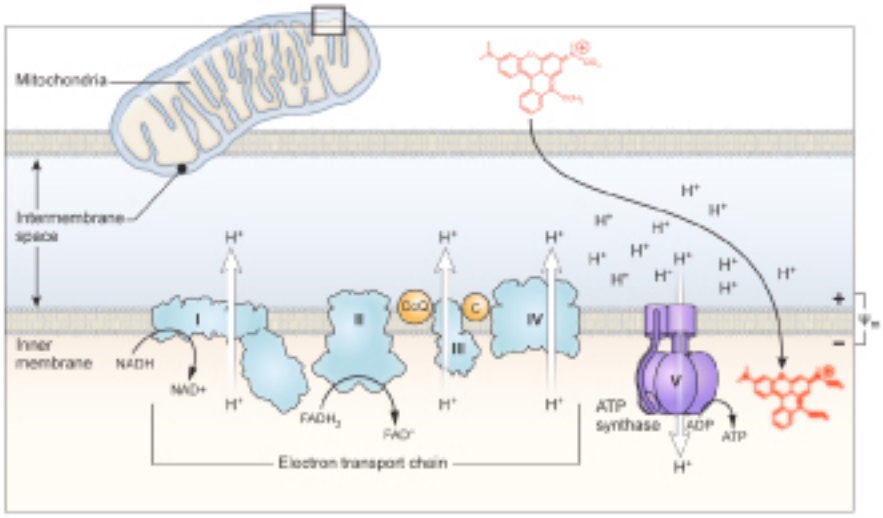

Figure 1.2.1 The Mitochondrial Bioenergetics. The electron transport chain protein complexes are responsible for creating the membrane potential of the mitochondria critical for its function and vitality

Chapter 2: Graphene

2.1 Structure of Graphene

Graphene is a crystalline allotrope of carbon with 2D properties. Carbon atoms are bonded through in-plane α bonds and perpendicular π orbitals. Bi-layer graphene consists of more than two layers of the 2D graphene. It is essentially an atomic scale hexagonal lattice made of carbon atoms. Graphene's stability is a result of its tightly packed atoms and sp^2 hybridization. Due to its atomic structure, practically every carbon in the hexagonal graphene sheet is available for chemical reaction from both sides (given the 2D form). The atoms on the edges, on the other hand, have some special chemical reactivity. However, perfectly flat graphene can be mostly chemically inactive.

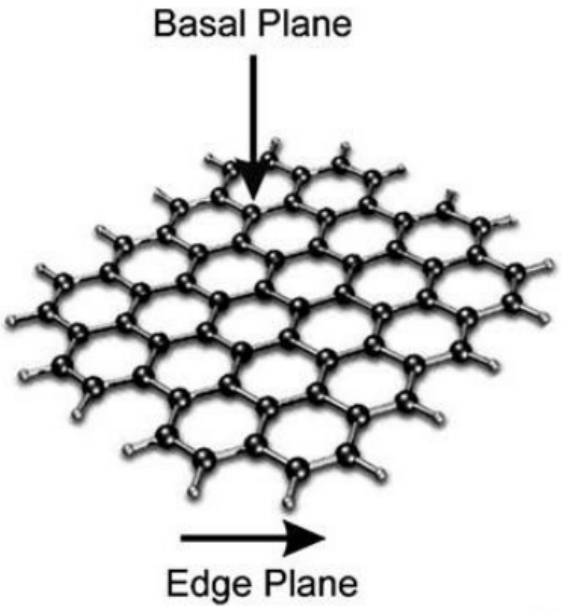

Figure 2.1.1 Single layer structure of graphene

2.2 Application & Properties of Graphene

Graphene is a zero-gap semiconductor, and it displays great electron mobility at room temperature. It has a lower resistivity than silver (lowest otherwise known at room temperature). Another highly applicable property of graphene is that it is optically transparent, rendering it very useful for optical and fluorescent microscopy, especially for biosensing. Thermal transport in graphene is an active area of research. It is reported that graphene has exceptionally large thermal conductivity of approximately 5300 $W.m^{-1}.K^{-1}$ at room temperature due to the graphene lattice waves by the substrate. The carbon-carbon bond length in graphene is about 0.142 nm. Its sheets can stack to form graphite. It is, mechanically, the strongest material ever tested with an intrinsic tensile strength of 130.5 GPa and Young's modulus of 1 TPa. Similar to other materials, certain regions of graphene are subject to thermal and quantum fluctuations in relative displacement.

A very important property of graphene is its biocompatibility. Researchers have been able to use graphene to create biosensors with epitaxial graphene on silicon carbide, which were capable of binding to antibodies[23]. There are even promises of application of graphene as in vitro sensors for future nanomedicine. However, there have been debates on the potential toxicity of graphene for health applications. Those largely depend on factors such as shape, size, purity, post-production processing steps, oxidative state, functional groups attached to the hexagonal surface, dispersion state, synthesis method (i.e. chemical vapor deposition), route, dose of administration and exposure time.

Given all the wonderful properties of graphene, it has found application in numerous industries, including solar cells, light emitting diodes (LED), touch panels and

smart windows and phones. Due to its 2D structure, it is also highly valuable in any flexible devices industries.

Chapter 3: Dyes

3.1 TMRE

A commonly used dye is tetramethylrhodamine Ethyl Ester (TMRE), which is a positively charged dye, passes through the cell membrane, accumulates in the mitochondria due to their negative charge and shows fluorescent staining at around the red spectra. It is cell permeant but does not aggregate in the cell membrane. However, depolarized or inactive mitochondria that have lower membrane potential as a result are not able to sequester TMRE dye, as a result, the fluorescent intensity drops as the membrane potential of the mitochondria drops. This is especially useful when studying the various factors that impact and result from a change or essentially a drop in the mitochondrial membrane potential. A common agent that affects the membrane potential of the mitochondria and therefore reduces the TMRE signal is the uncoupling agent, FCCP, which was aforementioned.

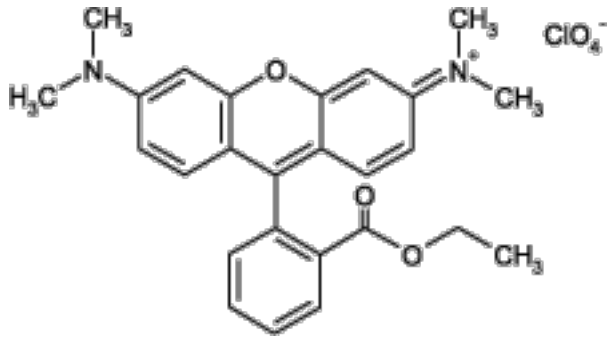

***Figure 2.3.1.1 The molecular structure of a TMRE dye** (3)*

3.2 MitoTracker Green

Another useful and applicable dye for our research purposes is the MitoTracker green fluorescent stain, which appears to localize to mitochondria regardless of their membrane potential. It is especially useful for locating these small organelles under fluorescent microscope for further studies. It has the excitation/emission of 419/516.

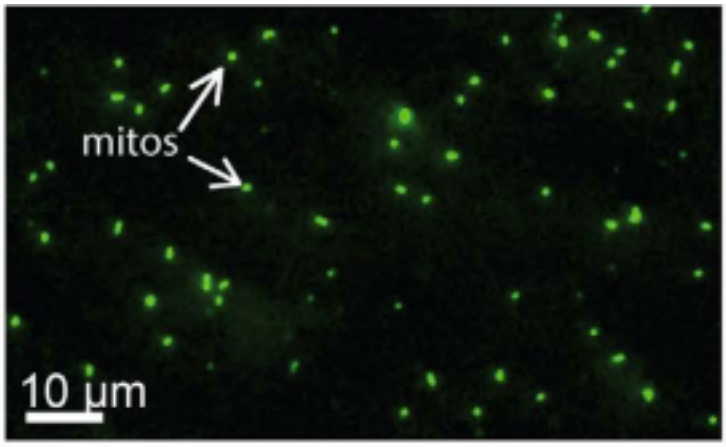

Figure 2.3.2.1 Image of isolated mitochondria tagged with MitoTracker Green[11]

Chapter 4: Carbon Nanotube Sensors

4.1 Structure & Properties

Carbon nanotubes are essentially graphene sheets that have been rolled up into cylindrical nanostructures. As a result they have unusual properties, which are extremely valuable in nanotechnology, electronics, optics and other fields of material science. The length to diameter ratio of nanotubes is around 132,000,000:1, significantly larger than any other material. This has lead to CNTs exceptional strength and stiffness along with its considerable electrical and thermal conductivity. CNTs can be either metallic or semi-conducting in their electrical behavior. Research at University of Pennsylvania suggested, "CNTs may be the best heat-conducting material man has ever known." It has also been shown that SWNT exhibit superconductivity below 20 degrees K. the small diameter and high aspect ratio, as previously discussed, is very favorable for field emission.

Figure 4.1.1 Single Walled Carbon Nanotube [4]

CNTs have widely been as transistors due to their size and structure. CNTS open a large range of applications in material science, electronics, chemical processing, energy management, and many other fields. Given a large portion of the human body is made up of organic carbon, CNTs, similar to graphene, could have extensive biomedical applications. There have been studies that showed cells are able to grow on nanotubes and there appears to be any toxic effect from these substrates. They also do not adhere to CNTs, leading to potential applications in coatings for implants and prosthetics, etc. there are already CNT based air and water filtration systems developed by many companies and research labs. These filters not only are capable of blocking very small molecules from passing, they also have antibiotic effects by killing the airborne and waterborne bacteria. Furthermore, there is a plethora of other applications for CNTs including solar collection, nanoporous filters, and various coating applications.

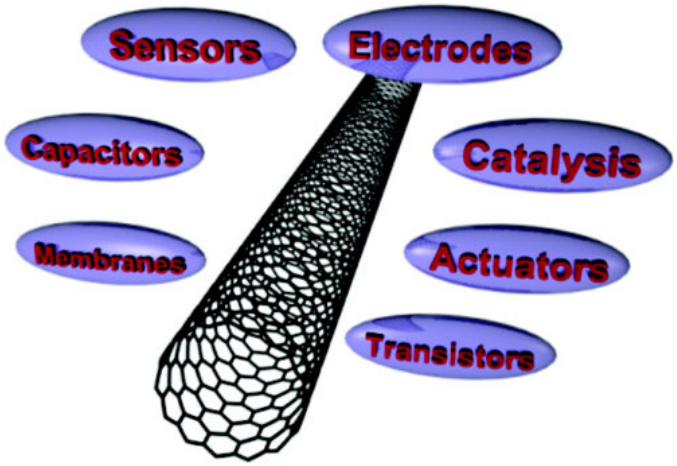

Figure 4.1.2 Many Applications of Nanotube Across Various Industries [5]

Chapter 5: Scanning Microwave Microscopy

5.1 Atomic Force Microscopy (AFM)

AFM is a probe-based microscopy that is designed to measure the local properties such as height, friction, magnetism etc of a substrate. It does so by measuring force between the probe, typically a pointy tip of 3-6 um height, and the sample.

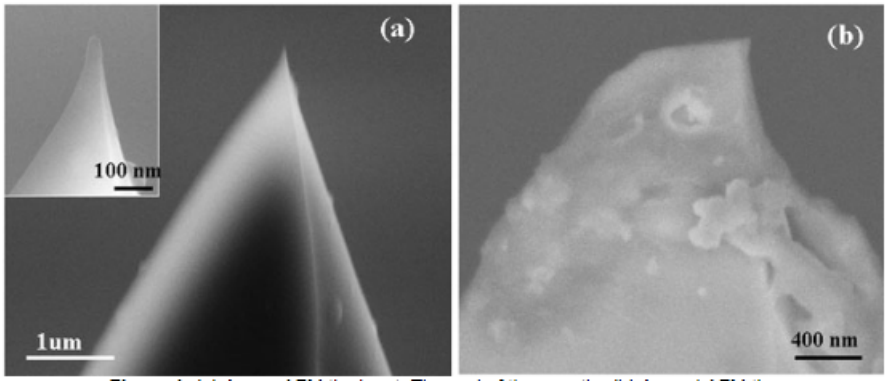

Figure 5.1.1 A new (a) versus a used (b) AFM Tip [6]

AFM operates by moving the tip along the surface of the substrate, either via contact mode or tapping mode (depending on the sample of study). A laser beam is reflected off the cantilever and hitting a position sensitive photo-detector. Following is a simplified diagrammatic representation of the AFM fundamentals.

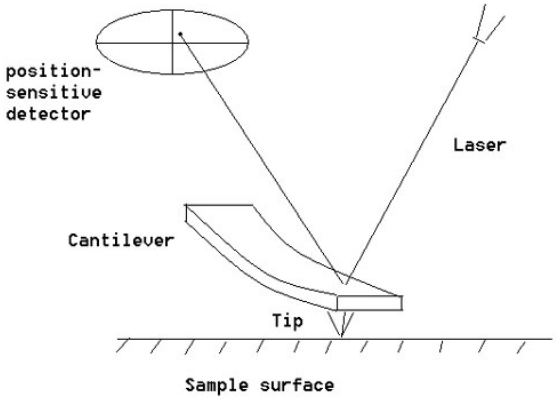

Figure 5.1.2 AFM with an optical lever [6]

As previously mentioned, there are various modes for an AFM tip for raster scanning. In contact mode, AFM machine uses a feedback loop to regulate the force exerted on the sample. In tapping mode, the tip touches the sample for only a short time, avoiding too much lateral force. This process uses amplitude modulation detection with a lock in amplifier. While direct force is measured in contact mode, that is not the case for tapping mode. This mode allows for more sensitive nano-imaging, for example for biological vital material.

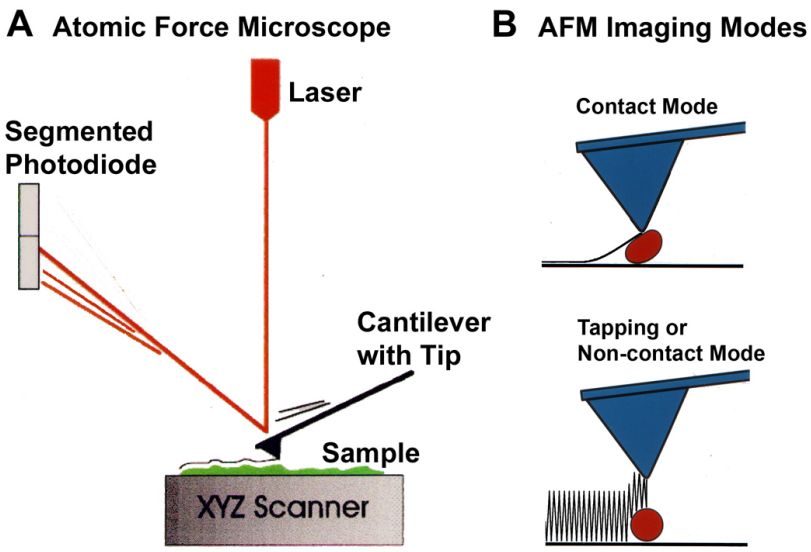

Figure 5.1.3 Various AFM Imaging Modes [7]

5.2 Scanning Microwave Microscopy (SMM)

Scanning microwave microscopy was developed after the invention of AFM. In this technique, microwave is used as the medium and electromagnetic interactions of the microwave from the probe and the sample are measured on nanoscale. AFM based SMM uses a metal or metal-coated probe. For the purposes of semiconductor researches, scanning capacitance microscopy are applied.

The Agilent Scanning microwave microscope consists of an AFM interfaced with a vector analyzer. This device works when a microwave signal is sent directly from the network analyzer and transmitted to a conductive AFM probe that is in contact with the sample. The reflected microwave is further detected by the same probe and sent to network analyzer. By measuring the S11 parameter of the (complex reflection coefficient) network analyzer we can map the impedance of the sample at the points of the tip contact [8].

5.3 Liquid Imaging with AFM

AFM machines are the only instruments capable of nanoscale liquid imaging. They do so by utilizing liquid cell compartments, which holds the sample as well as the probe during imaging.

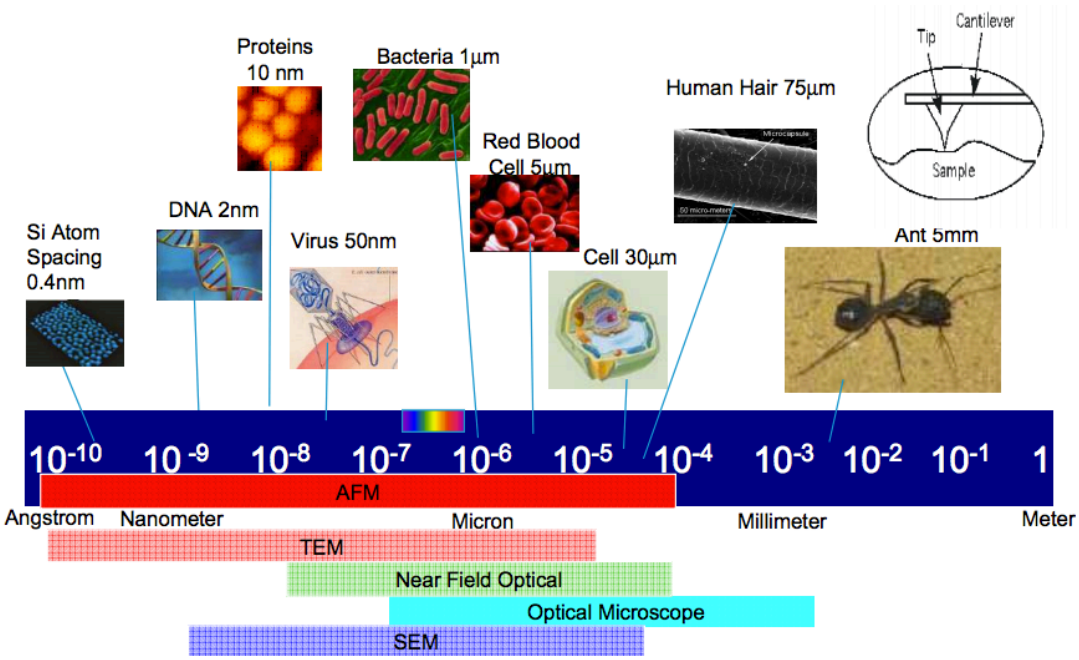

Figure 5.3.1 The Many Applications for Liquid Cell Imaging (Agilent)

5.4 SMM imaging of Mitochondria

Similar to bacterial quorum sensing, mammalian mitochondria participate in inter-organelle communication. One study (Wallace et al) showed that mitochondria align along the cristae, though the exact mechanisms of communication is not yet fully known. Previously, SMM imaging has been done on E-coli and CHO cells[22]. Using this technique, the GHz capacitance between a tip and the sample under study (i.e. mitochondria) can be measured with nanoscale resolution and high accuracy.

5.4.1 SMM Imaging in liquid

The same concept applied to AFM imaging in liquid can be applied to SMM imaging in liquid. The set up is the same and liquid cells can be used to hold down the biological sample within the appropriate media. However, when the AFM tip is immersed in water there are noticeable changes.

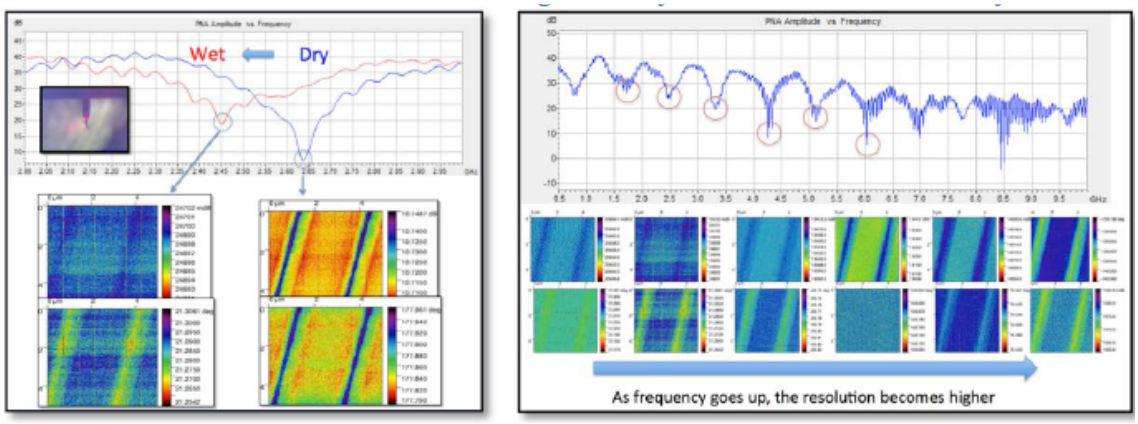

Figure 5.4.1.1 SMM in liquid with contact mode, and the resolution dependence on measurement frequency.

When a tip-sample set up is immersed into water or any other liquid medium, there are noticeable changes. As the above figure suggests, the S11 spectrum is shifted to the left. The lateral spatial resolution is reduced; likely since the microwave field near the tip is more diffused in water. We also observed that when the microwave frequency goes up, there is a trend that the SMM resolution increases.

Chapter 6: Materials & Methods

6.1 Materials

My research is two fold. First, I will discuss the materials used for the optimization techniques in CNT deposition and functionalization for the purposes of biosensor development. Secondly, the preliminary studies on SMM imaging of isolated mitochondria tethered to the surface of previously developed graphene devices will be discussed.

6.1.1. CNT Deposition Optimization Technique

For CNT deposition and wafer quality optimization, we used three different methods for the dissolution of polycarbonate filter papers that are commercially available by Millipore:

1. Dichloromethane - low boiling point
2. Chloroform – low boiling point
3. N-Methyl-2-pyrrolidone (NMP) – high boiling point

Milipore's Polycarbonate Filter Paper

Filter papers were dissolved using the above solvents in the vacuum filtration technique of pure nanotubes and transferred onto 1 mm glass substrates. The nanotube wafers were then characterized via scanning electron microscopy (SEM) and atomic force microscopy (AFM) to confirm their quality, cleanliness and properties. Various functionalization schemes were also explored in order to optimize the tethering protocol on nanotubes.

6.1.2 Scanning Microwave Imaging of Isolated Mitochondria

As previously discussed, the intricate mitochondrial pathways revolving around metabolism, signaling, cristae remodeling, and apoptosis are not yet fully understood, and this lack of knowledge can be largely attributed to lack of measurement technologies, mostly due to the micro and nanoscale size of these organelles. It is known that Transmission Electron Microscopy (TEM) only acquires a snapshot in time of a fixed sample. And optical fluorescent microscopy cannot capture an image of the inner workings of the mitochondria. For this project, we used our Keysight's Scanning Microwave Microscope (15/16smm). This is one of the only two machines in the world capable of SMM liquid imaging of vital samples. We have demonstrated an absolute capacitance measurement of ~ aF of uncertainty. The local impedance of sample is estimated by measuring the reflection of the microwave at tip-sample interface using a VNA and calibrated using, for example, a standard impedance sample.

Olympus fluorescent light source was concurrently used in the AFM/SMM machine to measure the fluorescent change of isolated mitochondrial from TMRE dye. This concept serves as proof of life for simultaneous SMM imaging. Mitochondrial isolation, device fabrication, functionalization and tethering are all discussed in the proceeding chapters.

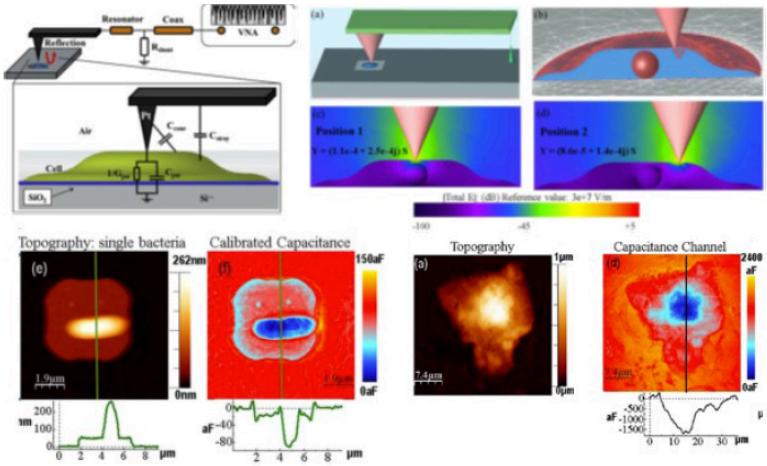

Figure 6.1.2.1 Scanning Microwave Microscopy of E-Coli and CHO Cells by Keysight

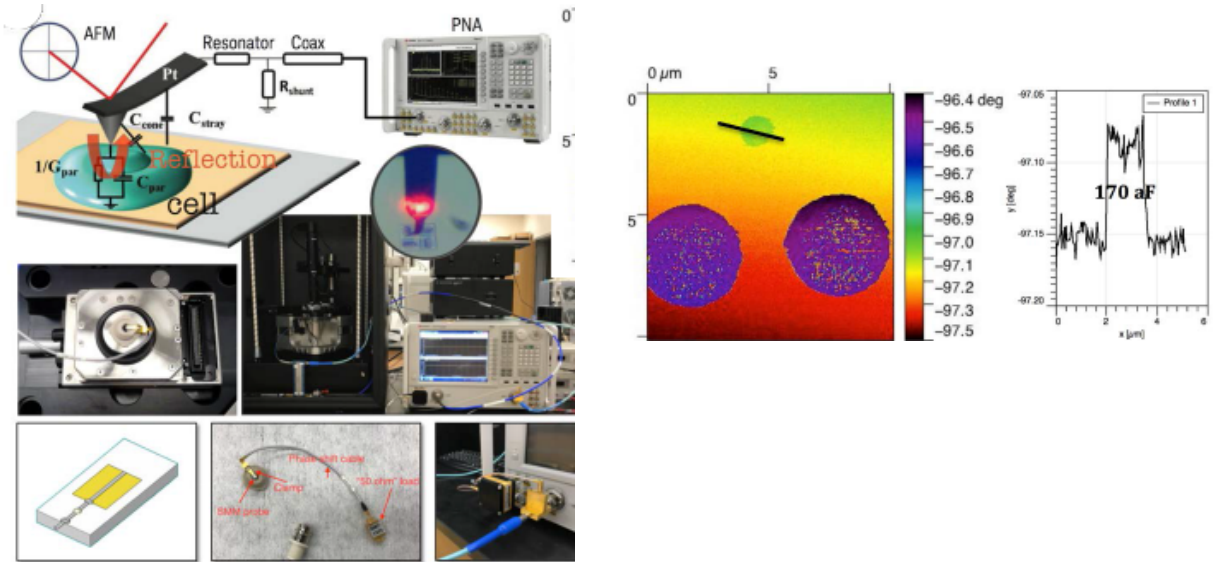

Figure 6.1.2.2 Upper Panel: the Diagram 1 and image of the SMM machine. Bottom Panel: The microwave probe, the front parts of the transmission line (including the clamp, the phase shift cable and the impedance match load), and the back-end part.

6.2 Methods

6.2.1 CNT Deposition Optimization Techniques

CNTs can be grown as both metallic and semiconductors. Vacuum filtration technique was used in order to deposit CNTs on top of filter paper. 200 μL of sonicated CNTs were poured on top of the filter paper on vacuum beaker. Once drained, isopropanol was added to the filter in order to wash away the surfactant. DI water was added to further wash the filter paper. The film (paper & CNT) is then dried and left at room temperature for future use. The filter paper is further baked in the oven at 60 degrees Celsius. CNT films are then transferred onto glass substrates and through a series of heating in a beaker with very specific timings, the filter paper is dissolved leaving pristine nanotubes on the surface of the glass substrate. The same process can be applied to silicon substrates for various imaging purposes.

6.2.2 CNT Characterization via SEM

In order to decide whether or not different types of solvents affect the cleanliness of the nanotubes, we used SEM imaging to see the distribution, density, and uniformity of the nanotubes. We used the UC Irvine LEXI (Laboratory for Electron and X-ray Instrumentation) facility for SEM imaging. The glass slides were then imaged via our Keysight Atomic Force Microscope to further characterize the properties of single nanotubes.

6.2.3 PDMS preparation

Silicone elastomer base were mixed thoroughly with curing agent (10:1 dilution) and the mixture was degassed for 30min in a vacuum chamber. PDMS was then poured on top of silicon wafer and baked in an over at 60˚ C for 1-2 hours

6.2.4 Transfer Method of Graphene Film

The members of the lab provided chemical Vapor Deposition (CVD) grown graphene on copper foil. Briefly, a 5 cm x 5 cm copper foil containing CVD grown single-layer graphene on one side was cut into 0.6 cm x 1.0 cm sheets. The side of the sheet containing graphene was pressed lightly against a block of pre-cured PDMS. The Cu-graphene-PDMS structure was then placed and left floating in a Cu-etchant bath (5 mg/ml ammonium persulfate in DI water) overnight in order to fully etch the copper away, leaving a pure layer of graphene on the surface of the PDMS slab.

6.2.5 Transferring of Graphene onto Glass Slides

Once copper is etched away and graphene has been fully and successfully transferred onto PDMS molds, we further transferred the graphene layer onto a silicon or glass substrate in order to make the device. The graphene-PDMS structure was then washed three times with DI H_2O for an hour in order to eliminate any residual ions from the copper-etching step. The wet PDMS/graphene block was then pressed against a 1-mm thick pre-cut glass slide that had been cleaned for one hour with 1:3 (v/v) H_2O_2: H_2SO_4 piranha solution. The glass-graphene-PDMS slide was kept under a slight pressure overnight to promote graphene-glass adhesion and allow the interfacial water to

evaporate. When the device was completely dry, the PDMS was carefully peeled off, leaving large-area single-layer graphene on the glass slide.

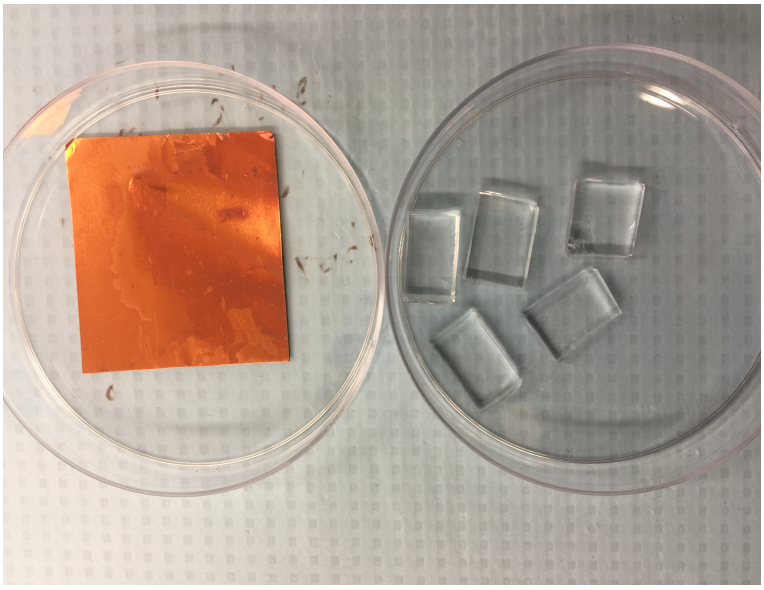

Figure 6.2.5.1 CVD Grown Graphene on Copper (left) and Graphene Transferred Onto PDMS Slabs After Etching (right)

6.2.6 Preparation of Buffers

Before the isolation of mitochondria from Hela cells, incomplete H buffer comprised of 5% BSA solution, respiration buffer as well as 200 uL of protease inhibitor were prepared. Incomplete H buffer was a mixture of 210mM mannitol, 70mM sucrose, 1mM EGTA, and 5mM HEPES. PH of the solution was adjusted to 7.2 by adding enough KOH. The incomplete H buffer was then mixed with 5% BSA solution to make a complete H buffer (10:1 dilution). The respiration buffer is made of 225mM mannitol, 75mM sucrose, 10mM KCl, 10mM TrisHCl, and 5mM KH2PO4. Afterwards, the PH of the solution was adjusted to 7.2 by adding enough KOH. These metabolites are involved

in mitochondrial respiration and as a result maintain mitochondrial functionality and vitality by sustaining its function.

6.2.7 Isolation of Mitochondria

HeLa cells were seeded in t75 flasks 3 days before isolation. On the day of isolation, approaximately 16 million cells were incubated with Mitotracker green and/or TMRE stains ~30 minutes prior to trypsinization. After treatment with trypsin, growth media was added to the mixture to stop the function of this protease. The cells were then centrifuged at 500 g to separate from the media. H-buffer was then added to the pellet followed by mechanical homogenization for 30 s. This process ensures the lysis of the cell membrane and release of the cytosolic components. From this step on the process involves a series centrifugation steps that would essentially separate these micron-sized organelles from the rest of the cellular components. Although not perfect, we do obtain enough mitochondria to test our device and model.

6.2.8 MitoTracker Green & TMRE Preparation

MitoTracker green fresh stock is prepared with DMSO and 1 μL of the aliquot is added per 10 mL of media into the flask. The cells are then incubated for 30 minutes in the incubator prior to isolation. Care was taken to not expose the solution with the dye to ambient light as that could lower the potency of the fluorescent dye.

TMRM kit was purchased from Sigma-Aldrich. The content of stock vial were mixed with 100μl of DMSO. The stock solution was then diluted with 1X PBS, or cell media to achieve a 10μM concentration. TMRE dye was then added to enough media containing the isolated mitochondria in order to bring the final concentration to 20-200

nM, generally 40 nM. The mitochondria were then incubated for 30 minutes at 37° C in the dark in order to avoid any fluorescent activation of the dye prior to imaging.

6.2.9 Graphene and CNT Functionalization

Graphene and/or CNT functionalization were carried out using a series of solution deposition, incubation and wash steps. First, 3.81 mg of pyrene-NHS was mixed with 2 mL dimethylformamide (DMF), and added to the PDMS chamber of each graphene device. Incubation with pyrene-NHS ensued for one hour at room temperature. The device was then washed sequentially with fresh DMF, DI water and PBS pH 7.2. Anti-TOM20 antibody (Santa Cruz Biotechnology) solution is added at 33.3 ug/mL concentration and incubated overnight at 4°C inside the desiccator. After two wash steps with PBS then DI H_2O, 0.1 M ethanolamine diluted in DI H_2O was added and incubated for one hour at room temperature then washed with DI H_2O. The next incubation with 0.1% TWEEN-20 was set for one hour at room temperature to deactivate the exposed graphene area by preventing unspecific protein adsorption. The functionalization scheme was partially adapted from. Finally, the devices were washed with DI H_2O then KCl buffer for immediate use.

6.2.10 Mitochondrial Tethering

Once the devices are [fabricated] and prepared, vital isolated mitochondria, kept in respiration buffer on ice, were added to the surface of the functionalized graphene. The set was then incubated for 15 minutes in 4 degrees in order to allow enough time for the mitochondria to bond to the Anti-TOM20 antibodies. Following this, the devices are washed gently with KCL buffer in order to rid the surface of the devices from any compounds except for tethered isolated mitochondria.

6.2.11 Fluorescent Imaging of Isolated Mitochondria

Initially, isolated mitochondria were kept in respiration buffer-in order to continue their functionality- and fluorescent imaged in a small petri dish. As aforementioned, MitoTracker green dye tags both the live and dead mitochondria alike, however TMRE dye only accumulates in the negatively charged matrix of the vital mitochondria. Time lapse imaging of TMRE intensity was measured in healthy mitochondrial sample versus those treated with the uncoupling agent FCCP. A drop in TMRE signal was detected and recorded within 100 ms.

Using an Olympus IX71 inverted microscope with two LED excitation sources (490nm & 565 nm), we observed the red and green fluorescence signals from MitoTracker Green FM and TMRE. Our field of view from our 20X objective is 200 μm x 300 μm, and we monitored the fluorescence from this field of view by controlling the microscope with NIH Micromanager software, which also set the exposure time to one second.

To process and analyze the images, ImageJ software was used. For the entire field of view analysis, we measured the fluorescence intensity from the field of view. In contrast, for single mitochondrion analysis, we defined regions of interest (ROI) enclosing the mitochondria and three more identical copies of that region of interest to define the background noise. We then assigned the fluorescence signal of the mitochondria as the measured signal subtracting the noise average.

Chapter 7: Results & Conclusion

7.1 CNT Deposition SEM

The different types of solvents for polycarbonate membranes did not differ that much in cleanliness. However, the type of substrate used did impact the general distribution and cleanliness of nanotubes.

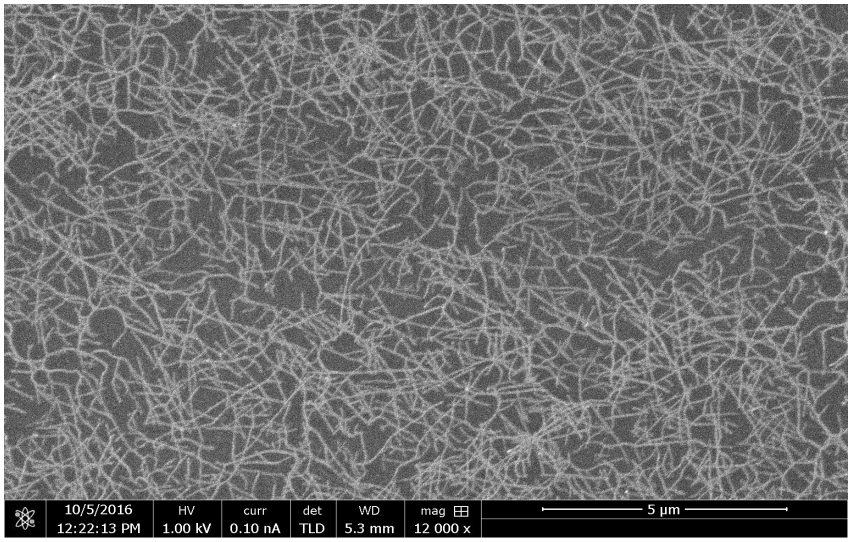

Figure 7.1.1 CNT on Glass Substrate 12,000 Magnitude

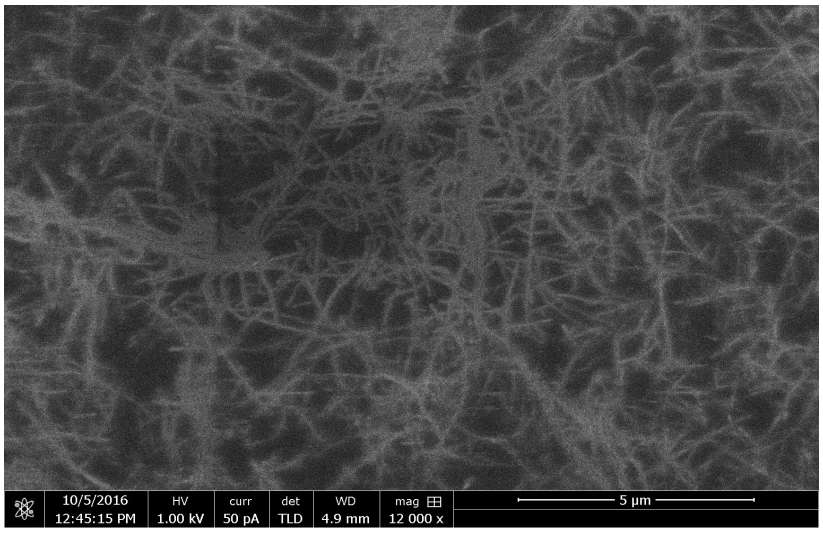

Figure 7.1.2 CNT on Quartz Substrate 12,000 Magnitude

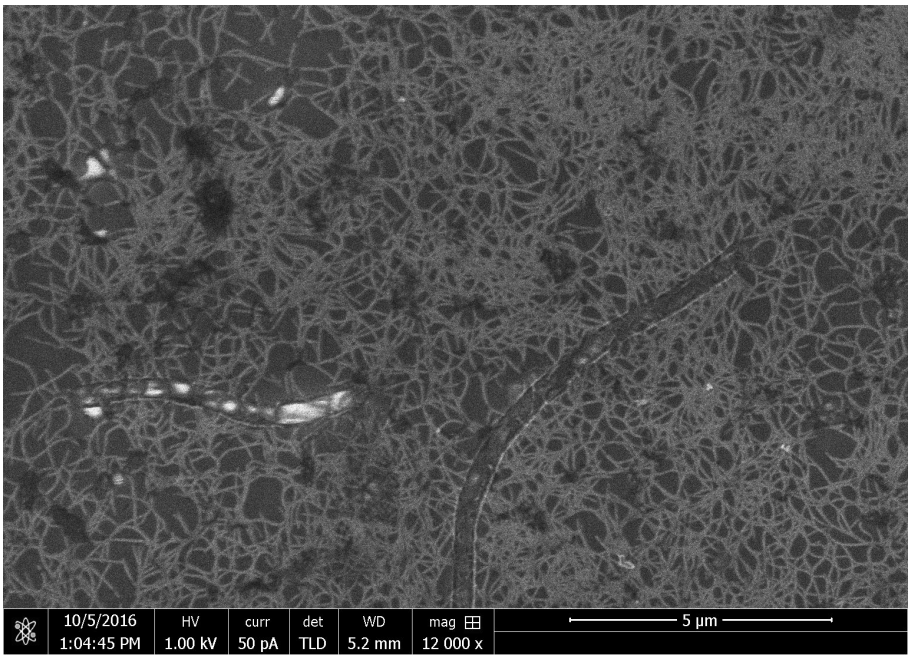

Figure 7.1.3 CNT on Polycarbonate Glass Substrate 12,000 Magnitude

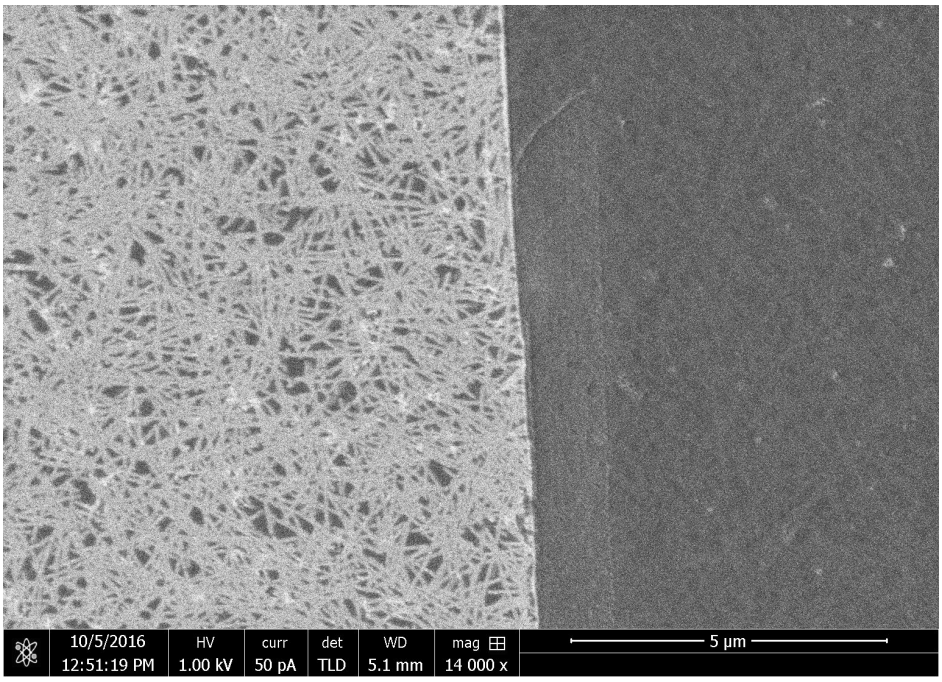

Figure 7.1.4 CNT on Silicon Substrate 14,000 Magnitude

7.2 Isolated Tethered Mitochondria- MitoTracker Green

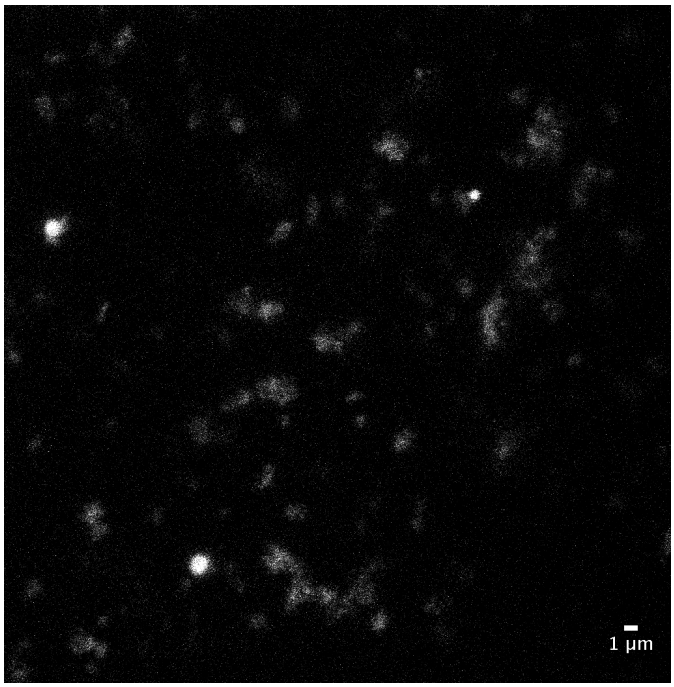

Figure 7.2.1 Bright Spots ~ 1.5 um in diameter are the isolated mitochondria Other bright dots are likely the background noise or unwashed dye molecules

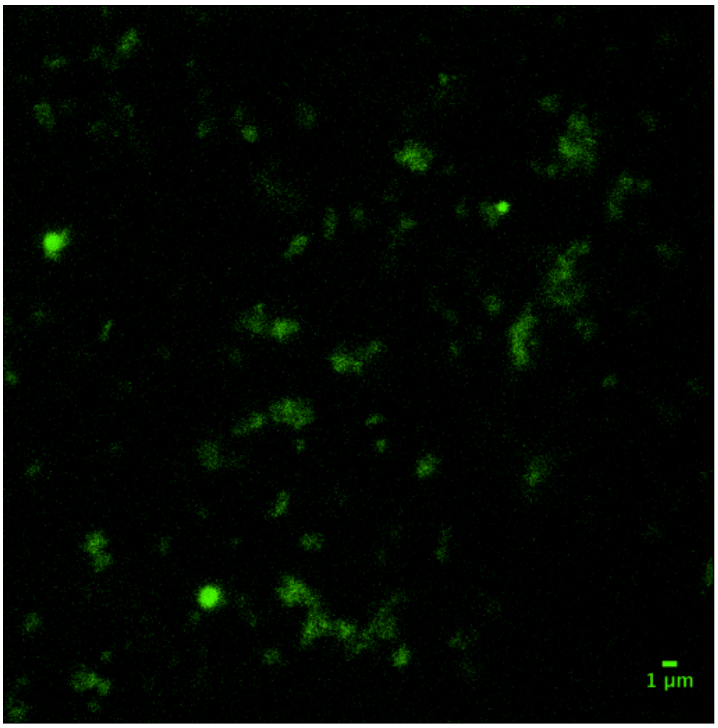

Figure 7.2.2 Isolated mitochondria in bright green-Mitotracker Green Dye (Image above edited via ImageJ Software)

7.3 Isolated Tethered Vital Mitochondrial- TMRE Dye

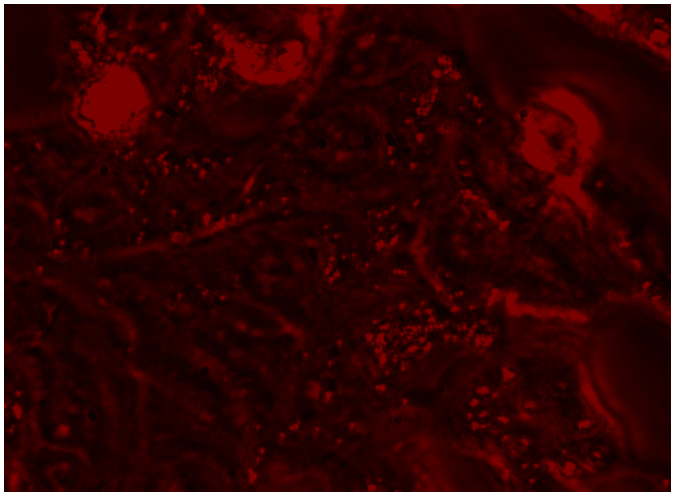

Figure 7.3.1 TMRE 60x 200ms 565nm 2-color

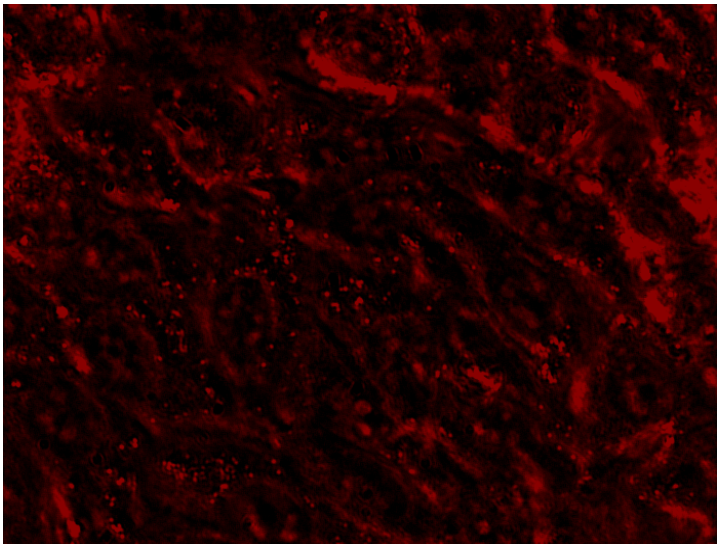

Figure 7.3.2 TMRE 60x 200ms 565nm-color

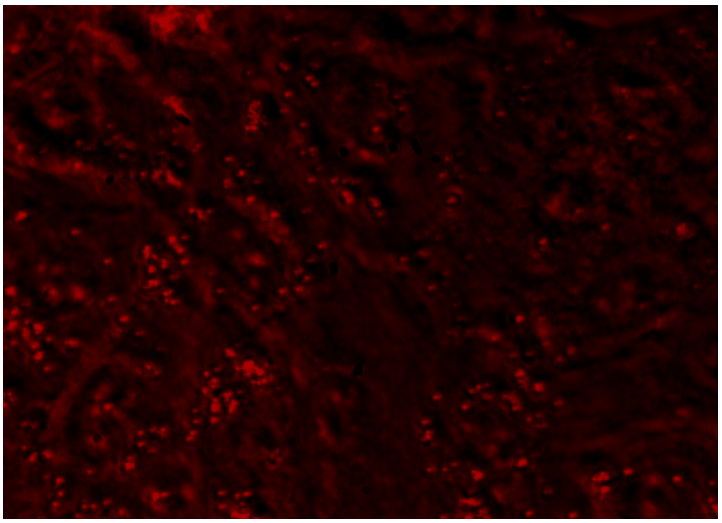

Figure 7.3.3 TMRE 60x 100ms 4bin 565nm-color

Shorter Exposure Time. The focus is not very high in most of the images, which can be improved via improvement in binning, time exposure, etc
However, the mitochondria are clearly stained and their viability evident due to the presence of membrane potential (TMRE).

7.4 SMM Imaging of Isolated Mitochondria

We have tethered vital isolated mitochondria on the surface of (graphene) solids (i.e. glass, silicon) and imaged them with scanning microwave microscope at 7 GHz. As a result, we obtained a crude uncalibrated capacitance map of single vital mitochondria as seen below. However, this map only yields capacitance information and does not reveal information about the mitochondrial morphology, more specifically the cristae (inner membrane) morphology. We aim to study that in more depth and develop platforms and techniques that would yield such data, preferably simultaneously.

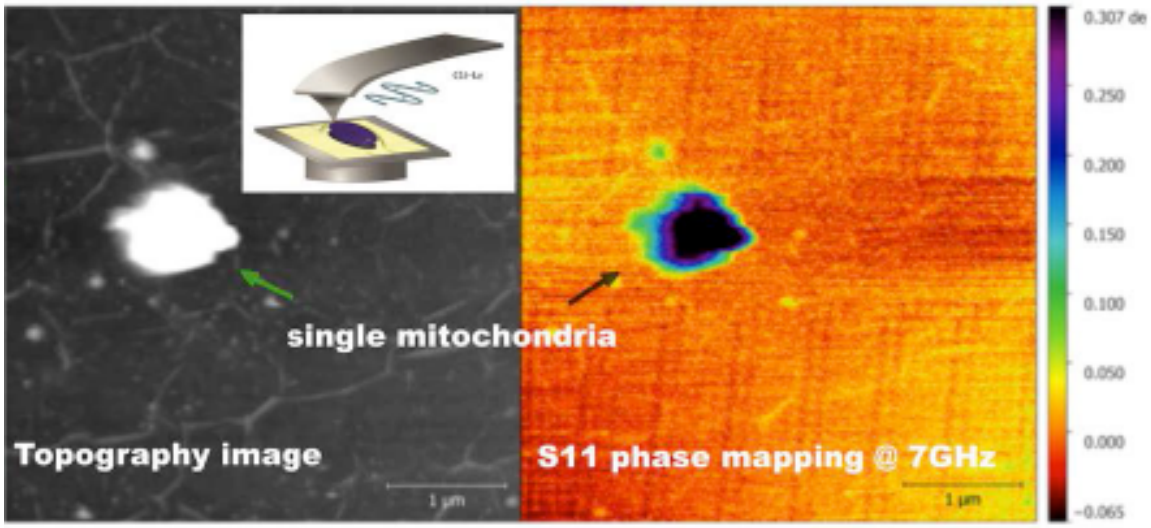

Figure 7.4.1 Topological image & the microwave impedance mapping of live mitochondria on graphene in liquid

7.5 Discussion & Future Directions

For CNT deposition experiments, we observed that the various solvents do not differ significantly in the cleanliness of the final deposited nanotubes. However, given their different properties, such as boiling points and toxicity, we could optimize the process by choosing the more efficient solvent. We did, however, notice changes in CNT uniform distribution, proper stacking, etc when using various materials as substrates. As is evident from the SEM images glass and quartz substrates yield better nanotube distributions while polycarbonate glass. However, it is possible to fabricate much cleaner nanotube devices using the spin coating technique. However, the focus of our experiments was on vacuum filtration techniques of CNT deposition.

On the other hand, using the SMM techniques previously mentioned, we can measure cristae remodeling and CytC release simultaneously as the membrane potential is dissipated via uncoupling agents (i.e. FCCP). This can be used to test whether or not a drop in membrane potential would in fact cause cristae remodeling in vital mitochondria. Furthermore, BID and BH3 mimetics will be used to induce MOMP (mitochondrial outer membrane permeabilization) to further test the model. BID and BH3 are known pro-apoptotic peptides and their roles can be studied in more depth using our technology.

During my research on various types of biosensor development, we have primarily worked on optimizing the sensor platforms. Given the tremendously small size of the sensing material and target molecules, it is crucial to ensure the functionality and efficiency of these platforms through consistent characterization methods (i.e. SEM, AFM, Raman, etc) as well as consistent end results. I aim to continue this work in the

Bio-Nano group for my PhD thesis and not only provide more robust proof of life data simultaneous to SMM imaging, but to extrapolate this model to intact cells in vivo where potential electromagnetic intracellular/intercellular communications are at play. I hope to be able to use the available advanced tools and nano-technology in order to shed some light on the intricate and complex cellular pathways surrounding the mitochondrial function with respect to various disorders and cancer.

References

1. Molecular Expressions (2015, November 13). Mitochondria. Retrieved from https://micro.magnet.fsu.edu/cells/mitochondria/mitochondria.html

2. Journals, Center for Cancer Research (2015, December). Identifying Stem Like Cells Using Mitochondrial Membrane Potential. https://home.ccr.cancer.gov/inthejournals/dev/itj_sukumar.asp

3. Quantitative measurement of mitochondrial membrane potential in cultured cells: calcium-induced de- and hyperpolarization of neuronal mitochondria: A. A. Gerencser, et. al.; J. Physiol. **590**, 2845 (2012)

4. "Carbon Nanotubes and Related Structures: New Materials for the Twenty-first Century", P. F. Harris, Cambridge University Press (1999) ISBN 0-521-55446-2

5. American Chemical Society. (2010, November 21). Emerging Applications of Carbon Nanotubes. Retrieved from http://www.nanowerk.com/news/newsid=19087.php

6. Wenji Mai (2017, September). Fundamental Theory of Atomic Force Microscopy. Retrieved from http://www.nanoscience.gatech.edu/zlwang/research/afm.html

7. Wen Zhang (2017, September). Retrieved from https://web.njit.edu/~wzhang81/

8. Wenhai Han (2008, June 16). Introduction to Scanning Microwave Microscopy. Retrieved from https://www.agilent.com/cs/library/applications/AN-IntroSMM_5989-8881.pdf

9. R. Saito *et al*. "Physical Properties of Carbon Nanotubes", Imperial College Press, 1998. ISBN 1-86094-093-5

10. Zand, K.; Pham, T. D. A.; Li, J.; Zhou, W.; Wallace, D. C.; Burke, P. J. "Resistive Flow Sensing of Vital Mitochondria with Nanoelectrodes". *Rev.* 2017.

11. Pham, T. D.; Pham, P. Q.; Li, J.; Letai, A. G.; Wallace, D. C.; Burke, P. J. "Cristae Remodeling Causes Acidification Detected by Integrated Graphene Sensor during Mitochondrial Outer Membrane Permeabilization". *Sci. Rep.* **2016**, *6*, 35907.

12. Sarosiek, K. A.; Chonghaile, T. N.; Letai, A. "Mitochondria: Gatekeepers of Response to Chemotherapy." Trends Cell Biol. 2013, 23, 612–619.

13. Hanahan, D.; Weinberg, R. "Hallmarks of Cancer: The next Generation.". Cell 2011, 144, 646–674.

14. Falchi, A.M., Isola, R., Diana, A., Putzolu, M., Diaz, G., 2005. Characterization of depolarization and repolarization phases of mitochondrial membrane potential fluctuations induced

15. Hashimoto, K., Rottenberg, H., 1983. Surface potential in rat liver mitochondria: terbium ion as a phosphorescent probe for surface potential. Biochemistry 22, 5738–5745.

16. Huser, J., Blatter, L.A., 1999. Fluctuations in mitochondrial membrane potential caused by repetitive gating of the permeability transition pore. Biochem. J. 343, 311–317.

17. Kroemer, G., Galluzzi, L., Brenner, C., 2007. Mitochondrial membrane permeabilization in cell death. Physiol. Rev. 87, 99–163.

18. Lim, T.-S., Davila, A., Wallace, D.C., Burke, P.J., 2010. Assessment of mitochondrial membrane potential using an on-chip microelectrode in a microfluidic device. Lab Chip 10, 1683–1688.

19. Lim, T.-S., Jain, D., Burke, P.J., 2011a. Biomembrane-gated carbon nanotube transistor as a sensing platform. In: Proc. 15th Int. Conf. Miniaturized Syst. Chem. Life Sci, pp. 1770–1772.

20. Lim, T.-S., Jain, D., Burke, P.J., 2011c. Protein nanopore-gated bio-transistor for membrane ionic current recording. In: Proc. 69th Device Res. Conf. 26. pp. 131–132.

21. Pham, T.D., Wallace, D.C., Burke, P.J., 2016. Microchambers with solid-state phosphorescent sensor for measuring single mitochondrial respiration. Sensors 1065, 1–14.

22. Maria Chiara Biagi, Rene Fabregas, Georg Gramse, Marc Van Der Hofstadt, Antonio Juarez, Ferry Kienberger, Laura Fumagalli, and Gabriel Gomila, 2016. Nanoscale Electric Permittivity of Single Bacterial Cells at Gigahertz Frequencies by Scanning Microwave Microscopy. ACS Nano, *10* (1), pp 280–288

23. Z Tehrani, G Burwell, M A Mohd Azmi, A Castaing, R Rickman, J Almarashi, P Dunstan, A Miran Beigi, S H Doak and O J Guy. 2014. Generic epitaxial graphene biosensors for ultrasensitive detection of cancer risk biomarker. 2D Materials 1 (2014) 025004